Simulation of Mach-Zehnder Interferometer plastic optical fibre for temperature and refractive index measurement

Ian Yulianti[1], N. M. Dharma Putra[1], Fianti[1], S. Maimanah[1], H. Rumiana[1], M. Y. M. Noor[2], A. S. M. Supa'at[2], O. Kurdi[3]

[1]Physics Department, Faculty of Mathematics and Natural Sciences, Universitas Negeri Semarang, Semarang, Indonesia
[2]School of Electrical Engineering, Faculty of Engineering, Universiti Teknologi Malaysia, Skudai, Johor Bahru, Malaysia
[3]Faculty of Mechanical Engineering, Universitas Diponegoro, Semarang, Indonesia

Corresponding e-mail: ianyulianti@mail.unnes.ac.id

Abstract. This work presents simulation of light propagation inside tapered structure- plastic optical fibre (POF) subjected to various surrounding temperatures and refractive index (RI). The tapered structure served as Mach-Zehnder interferometer (MZI) which split light into core modes and clad modes that recombined at the end of the taper. Simulation was done by using Beam Propagation Method (BPM) solved using Finite Difference Method (FDM). The light launched in to the MZI was varied from 611nm to 655nm. In order to give temperature effect, the temperature was varied from 30°C to 80°C with increment of 10°C. The results showed that the free spectral range (FSR) of the MZI are shifted as temperature increased. The sensitivity for the peak and dip of the FSR are -0.0158 nm/°C and -0.0153 nm/°C, respectively. For RI sensitivity investigation, the surrounding RI was varied from 1.333 to 1.349. The sensitivity of peak FSR and dip FSR to RI change are -98.638 nm/RIU and 105.4 nm/RIU. Therefore, the MZI can be used to measure RI and temperature simultaneously.

1. Introduction

Temperature and refractive index (RI) are important parameters in many applications such as biomedicine, biochemistry, food industry and environment. In chemical or food industry, temperature and RI measurement are used in quality control. Meanwhile, in environmental application, temperature and RI serve as indicators in assessing the level of pollution [1][2]. Therefore, researches have been conducted to develop temperature and RI sensor using various techniques. Among available techniques, optical fibre sensor is interesting since it is free from electromagnetic interference and also suitable for hazardous environment.

Temperature and RI measurement could be done simultaneously by modifying optical fibre structure and exploiting the measurement techniques. Zhang et al. [3] proposed optical fibre sensor using fibre Bragg grating (FBG) and Fabry-Perot interferometer (FPI) using single-mode silica optical fibre (SMF). Beside SMF, photonic crystal fibre (PCF) has also been used by modifying it in to D-shape and coating it by silver film so that it excite surface plasmon resonance (SPR) [4]. Moreover, the PCF was also filled by silver nanowire. The above-mentioned sensors rely on wavelength modulation technique. Other wavelength-based sensor for temperature and RI measurement was developed using microfibre

resonator and FBGs [5]. Wavelength-based sensor offers higher accuracy compared to intensity-based sensor since its measurement is independent from intensity fluctuation and loss. However, complex fabrication technique limits its advantages.

Wavelength-based sensor could also realize using Mach-zehnder interferometer (MZI). MZI has several advantages such as good linearity [6], low cost [7], compact size and easy fabrication process [8]. In-line MZI using polymer optical fibre (POF) has been proposed as RI and strain sensor by using simple fabrication technique [9]. Graded-index POF (GI-POF) was used to form the MZI by forming taper using heat-and-pull technique. It was shown that the sensor has sensitivity in the order of 10^{-1}pm and 10^1 nm for strain and RI, respectively. Due to the thermo-optic nature, MZI structure could also be employed for temperature measurement.

In this work, we studied the response of in-line MZI using step-index POF (SI-POF) to temperature and RI theoretically using numerical method. SI-POF was used since it has larger diameter and therefore sturdier than GI-POF. Larger diameter also makes SI-POF is easy to handle. The simulations were done by using Beam Propagation Method (BPM), which was solved numerically using Finite Difference Method (FDM) employing BeamProp software.

2. Sensor Working Principle

The in-line MZI structure consists of two tapers separated by an interferometry region with length of L, as shown in Figure 1. Light launched in to the MZI propagates in the core mode and when it passes through the first taper, some of the light refracted in to the cladding and propagates along the interferometry region. At the second taper, the cladding modes then recombine with the core modes. Due to the difference between RI of core and clad, the light travelled in both paths have a phase difference which further results in interference when the light recombines.
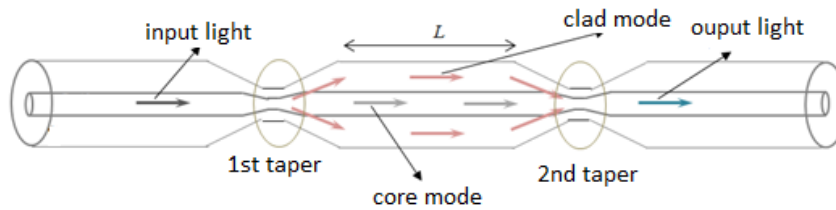

Figure 1. In-line MZI structure and light splitting inside it.

The intensity of the interference light is defined by [10]

$$I = I_1 + I_2 + 2\sqrt{I_1 I_2} \cos \Delta\phi \tag{1}$$

where I_1 and I_2 are the intensity of core modes and intensity of clad modes, respectively. $\Delta\phi$ is the phase difference between core modes and clad modes which is define by:

$$\Delta\phi = \phi_{core} - \phi_{clad} = \frac{2\pi\left(n_{eff}^{core} - n_{eff}^{clad}\right)L}{\lambda} = \frac{2\pi\Delta n_{eff}L}{\lambda} \tag{2}$$

where λ, n_{eff}^{core} and n_{eff}^{clad} are the light wavelength, the effective refractive index (ERI) of core and clad, respectively. Δn_{eff} is the difference between ERI of core and clad. When the phase difference satisfy $\Delta\phi = (2m+1)\pi$, $m = 0,1,2,...$, the interference light intensity reach a maximum value. The wavelength at which the maximum interference occurs is defined by [6]:

$$\lambda_m = \frac{\Delta n_{eff} L}{2m+1} \tag{3}$$

The free spectral range (FSR) between two maximum intensity is defined by

$$\text{FSR} = \lambda_m - \lambda_{m-1} \approx \frac{\lambda^2}{\Delta n_{eff} L} \tag{4}$$

where λ_m and λ_{m-1} are the mth and $(m-1)^{th}$ order of the peak wavelengths. From (4), it is clear that the FSR is depend on the ERI of both core and clad. The ERI of clad at tapered region is affected by the RI of the surrounding [6] and also by the temperature through the thermo-optic effect. Therefore, by observing the change of the FSR of the output spectrum, temperature and RI can be determined. However, since both temperature and RI contribute to the FSR, then we proposed to measure FSR of peak and dip. Therefore, using sensitivity of FSR of peak and FSR of dip to temperature and RI, simultaneous measurement of temperature and RI could be done.

3. Method

Prior to simulation, the in-line MZI was first fabricated using heat-pull method [9] using SI-POF with n_{core} of 1.49 and n_{clad} of 1.41. The POF core and clad diameter are 980 µm and 1mm, respectively. The thermo-optic coefficient (TOC) of the PMMA is $-1.2 \times 10^{-4} \, ^\circ C^{-1}$ [11]. The interference region (L) was set to be 2 cm. The waist diameter of the first and the second taper are 872 µm and 790 µm, respectively. Complete dimension specification is shown in Figure 2. To obtain the output spectrum, the light propagation inside the MZI was simulated with wavelength in the range of 611nm to 655nm. To investigate the response to temperature change, the surrounding temperature was varied from 30℃ to 80℃ with increment of 10℃, while the surrounding RI was maintained at air RI which is 1.0. Meanwhile, to obtain sensor sensitivity to RI change, the RI was varied from 1.333 to 1.349 which are the RI of glucose with various concentration [12].
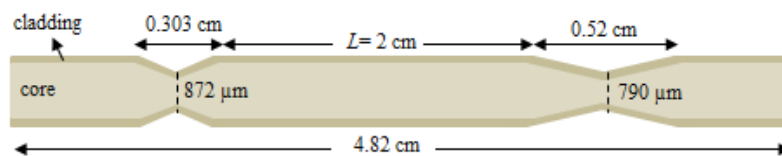

Figure 2. Dimension specification of MZI used in the simulation.

4. Results and Discussions

Simulation was done to obtain output spectrum of the MZI subjected to temperature and RI change. From the output spectrum, the FSR change was then obtained. By plotting the FSR of peak and FSR of dip to temperature and RI, the MZI sensitivity to temperature and RI were determined.

4.1. Temperature sensitivity

Light propagation inside MZI at temperature of 30℃ and wavelength of 650nm is shown in Figure 3(a). It is shown that as light propagates through the first taper, some of the light penetrates through the clad as shown by red colour that spread out to the core-clad interface at z of ~1.2 cm, as expected. The steep taper of the first taper caused refraction with high intensity at the core-clad interface. At z of around 3 cm at where the second taper located, the light interference occurs. The smooth structure of the second taper minimize refraction and contributes to the higher intensity of interference of core modes and clad modes [12]. The output spectrum at temperature of 30℃ is shown in Figure 3 (b).
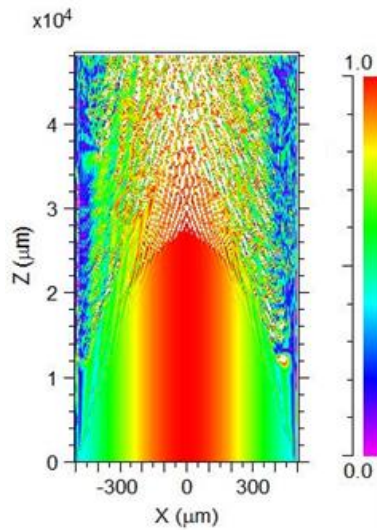
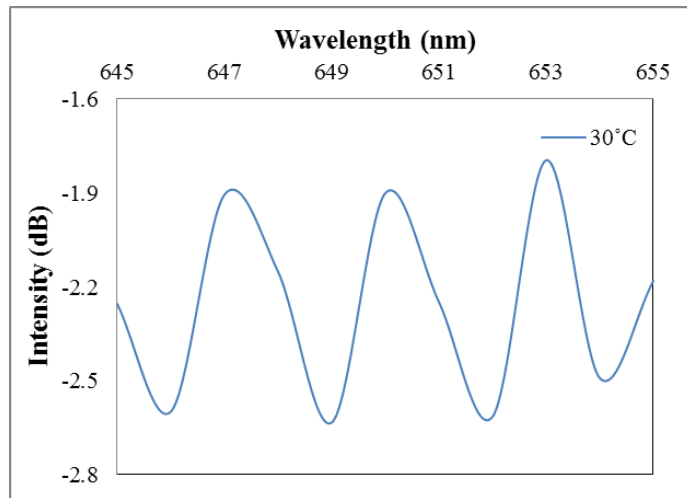**Figure 3 (a).** Light propagation inside MZI at temperature of 30ºC and wavelength of 650nm.

Figure 3 (b). The output spectrum at temperature of 30ºC.

The change of FSR of peak and dip were plotted against temperature value as shown in Figure 4. It is shown that as temperature increases, the FSR of both peak and dip decrease. The sensitivity of FSR of peak to temperature is -0.0158 nm/˚C with correlation coefficient of 87.83%. Meanwhile, for FSR of dip, the sensitivity is – 0.0153 nm/˚C with correlation coefficient of 94.9%.
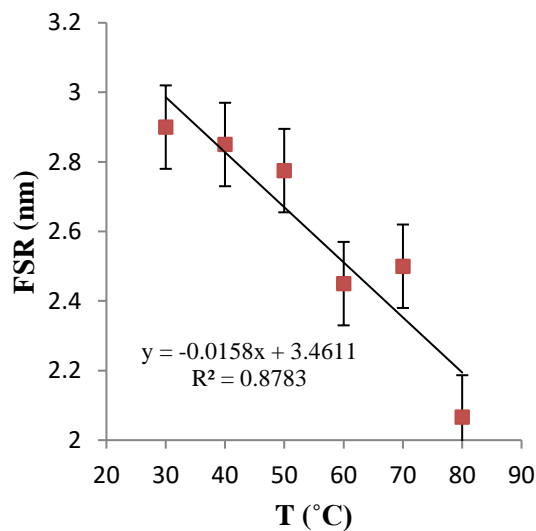

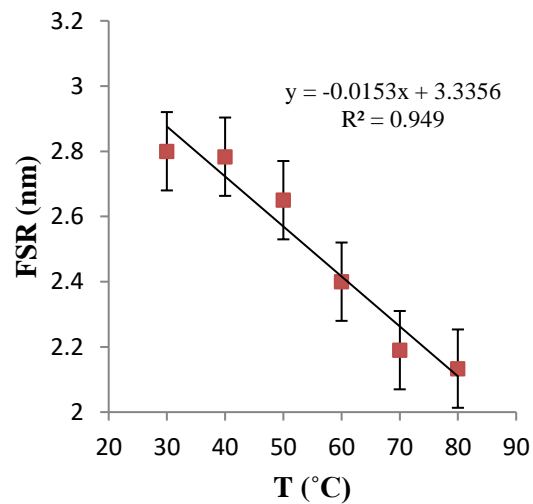**Figure 4 (a).** The change of FSR of peak.

Figure 4 (b) The change of FSR of dip.

∗The error bars represent the standard error of the data

4.2. RI sensitivity

For RI sensitivity investigation, the temperature was maintained at 28ºC. The change of FSR due to RI change of both peak and dip are shown in Figure 5. As response to temperature, it is also observed that the FSR decreases as RI increases. It was found that the sensitivity of peak FSR to RI change is -98.638

nm/RIU with correlation coefficient of 96.12 %. Meanwhile, higher sensitivity which -105.4 nm/RIU was obtained for dip FSR. However, linearity of dip FSR was lower compared to that of peak FSR as indicated by lower correlation coefficient which is 90.1 %. The sensitivity is higher than that of GI-POF based MZI [9].
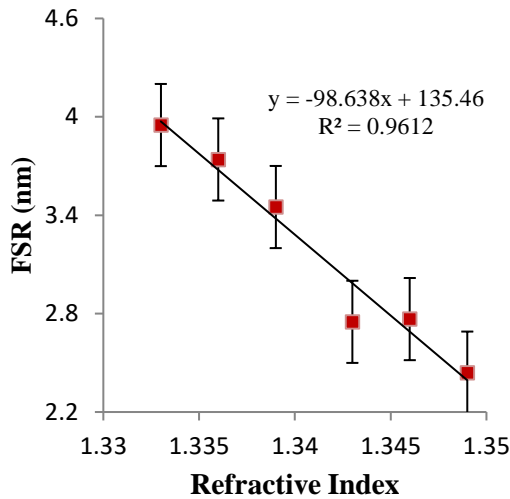

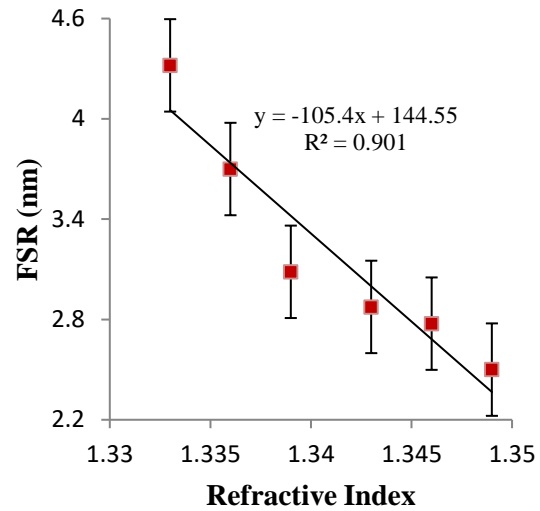**Figure 5 (a).** The change of FSR of peak.   **Figure 5 (b)** The change of FSR of dip.

* The error bars represent the standard error of the data.

4.3. Temperature and RI determination

Simultaneous determination of temperature and RI can be done by using sensitivity of FSR of peak and dip to temperature and RI. Since both FSR of peak and dip depend on temperature and RI, then the change of both FSRs can be defined by

$$\Delta \text{FSR}_p = \frac{\partial \text{FSR}_p}{\partial \text{T}} \Delta T + \frac{\partial \text{FSR}_p}{\partial \text{n}} \Delta n \tag{5}$$

$$\Delta \text{FSR}_d = \frac{\partial \text{FSR}_d}{\partial T} \Delta T + \frac{\partial \text{FSR}_d}{\partial n} \Delta n \tag{6}$$

where ΔFSR_p and ΔFSR_d are the change of peak FSR and dip FSR, respectively. $\frac{\partial \text{FSR}_p}{\partial T}$ and $\frac{\partial \text{FSR}_p}{\partial n}$, are sensitivity of peak FSR to temperature and RI, respectively. Meanwhile, $\frac{\partial \text{FSR}_d}{\partial T}$ and $\frac{\partial \text{FSR}_d}{\partial n}$ are sensitivity of dip FSR to temperature and RI, respectively. By using sensitivity obtained from the characterization, then equation (5) and (6) can be written as

$$\Delta \text{FSR}_p = -0.0158 \, \Delta T + (-98{,}638)\Delta n \tag{7}$$

$$\Delta \text{FSR}_d = -0.0153 \, \Delta T + (-105{,}4)\Delta n \tag{8}$$

Equation (7) and (8) can be written in matrix form as

$$\begin{bmatrix} -0.0158 & -98.638 \\ -0.0153 & -105.4 \end{bmatrix} \begin{bmatrix} \Delta T \\ \Delta n \end{bmatrix} = \begin{bmatrix} \Delta \text{FSR}_p \\ \Delta \text{FSR}_d \end{bmatrix} \tag{9}$$

Therefore, temperature and RI change can determine simultaneously by solving the matrix equation, as defined by

$$\begin{bmatrix} \Delta T \\ \Delta n \end{bmatrix} = \frac{1}{D} \begin{bmatrix} -105.4 & 0.0153 \\ 98.638 & -0.0158 \end{bmatrix} \begin{bmatrix} \Delta \text{FSR}_p \\ \Delta \text{FSR}_d \end{bmatrix} \tag{10}$$

where D is the matrix determinant.

5. Conclusions

Investigation of the sensitivity of in-line MZI based on POF to temperature and RI have been done numerically. The results showed that surrounding temperature and RI change the output spectrum of the MZI. In terms of FSR, the MZI has temperature sensitivity of -0.0158 nm/°C and -0.0153 nm/°C for peak FSR and dip FSR. It is also observed that the MZI has higher sensitivity to RI change. The sensitivity of peak FSR and dip FSR to RI change are -98.638 nm/RIU and 105.4 nm/RIU. By observing the peak FSR and dip FSR, simultaneous measurement of temperature and RI can be accomplished.

Acknowledgements

References
[1]   Harris J, Lu P, Larocque H, Chen L and Bao X 2015 *Sens. and Act. B: Chemical* **206** 246-251
[2]   Yao Q, Meng H, Wang W, Xue H, Xiong R, Huang B, Tan C, and Huang X 2014 *Sens. and Act. A: Phys* **209** 73-77
[3]   Zhang T, Liu Y, Yang D, Wang Y, Fu H, Jia Z, and Gao H 2019 *Opt. Fibre Technol* **49** 64–70
[4]   Zhao L, Han H, Lian Y, Luan N, and Liu J 2019 *Opt. Fibre Technol* **50** 165–171
[5]   Xiao Y Y, Cai X P, and Chen H 2019 *Optik (Stuttg)* **191** 116–120
[6]   Wang Q, Wang B T, Kong L X, and Zhao Y 2017 *IEEE Trans. on Instr. and Meas.* **9** 2483–2489
[7]   Ma Y, Qiao X, Guo T, Wang R, Zhang J, Weng Y, Rong Q, Hu M, and Feng Z 2012 *IEEE Sens J.***12** 2081–2085
[8]   Zhao N, Lin Q, Jing W, Jiang Z, Wu Z, Yao K, Tian B, Zhang Z, and Shi P 2017 *Sens. and Act.***267** 491-495
[9]   Jasim A A, Hayashi N, Harun S W, Ahmad H, Penny R, and Mizuno Y 2014 *Sens. Act. A: Phys* **219** 94–99
[10] Wang Q, Wei W, Guo M, and Zhao Y 2016 *Sens. and Act. B: Chemical* **222**159-165
[11] Luo Y, Yan B, Zhang Q, Peng G, Wen J, and Zhang J 2017 *Sensors* **17** 511
[12] Bhardwaj V and Singh V K 2016 *Sens. and Act. A: Phys* **244** 30-34